Fabrication of three-dimensional woodpile photonic crystals in a PbSe quantum dot composite material

Jiafang Li, Baohua Jia, Guangyong Zhou, and Min Gu

Centre for Micro-Photonics and CUDOS, Faculty of Engineering and Industrial Sciences, Swinburne University of Technology, Hawthorn, Victoria 3122, Australia
mgu@swin.edu.au

http://www.swin.edu.au/feis/cmp

Abstract: Incorporating active media into three-dimensional (3D) photonic crystals (PCs) is a useful step towards exploring the functionalities of PCs. Here we report, for the first time, on the fabrication of 3D woodpile PCs with a commercial PbSe quantum dot (QD) composite material by using the two-photon polymerization technique. The fabricated crystals possess photonic band gaps in the near-infrared wavelength region, which have a suppression rate of ~50% in the stacking direction, measured with an angle-resolved Fourier-transform infrared spectrometer. The woodpile structures fabricated under different conditions are also characterized by using a scanning near-field optical microscope, providing a useful feedback towards optimizing the fabrication of 3D woodpile PCs in QD composites.

OCIS codes: (220.4000) Microstructure fabrication; (999.999) Photonic crystals; (999.999) Nanocrystal quantum dots.

References and links

1. S. Y. Lin, J. G. Fleming, D. L. Hetherington, B. K. Smith, R. Biswas, K. M. Ho, M. M. Sigalas, W. Zubrzycki, S. R. Kurtz, and J. Bur, "A three-dimensional photonic crystal operating at infrared wavelengths," Nature **394**, 251-254 (1998).
2. S. Noda, K. Tomoda, N. Yamamoto, and A. Chutinan, "Full three-dimensional photonic bandgap crystals at near-infrared wavelengths," Science **289**, 604-606 (2000).
3. A. Blanco, E. Chomski, S. Grabtchak, M. Ibisate, S. John, S. Leonard, C. Lopez, F. Meseguer, H. Miguez, J. Mondia, G. Ozin, O. Toader, and H. van Driel, "Large-scale synthesis of a silicon photonic crystal with a complete three-dimensional bandgap near 1.5 micrometres," Nature **405**, 437-440 (2000).
4. S. Shoji and S. Kawata, "Photofabrication of three-dimensional photonic crystals by multibeam laser interference into a photopolymerizable resin," Appl. Phys. Lett. **76**, 2668-2670 (2000).
5. S. Wong, M. Deubel, F. Pérez-Willard, S. John, G. A. Ozin, M. Wegener, and G. Von Freymann, "Direct laser writing of three-dimensional photonic crystals with a complete photonic bandgap in chalcogenide glasses," Adv. Mater. **18**, 265-269 (2006).
6. N. Tétreault, G. von Freymann, and G. A. Ozin, "New route to three-dimensional Photonic Bandgap Materials: Silicon Double Inversion of Polymer Templates," Adv. Mater. **18**, 457-460 (2006).
7. M. Straub, and M. Gu, "Near-infrared photonic crystals with higher-order bandgaps generated by two-photon photopolymerization," Opt. Lett. **27**, 1824–1826 (2002).
8. M. Straub, M. Ventura, and M. Gu, "Multiple higher-order stop gaps in infrared polymer photonic crystals," Phys. Rev. Lett. **91**, 043901/1-043901/4 (2003).
9. K. K. Seet, V. Mizeikis, S. Matsuo, S. Juodkazis, and H. Misawa, "Three-dimensional spiral-architecture photonic crystals obtained by direct laser writing," Adv. Mater. **17**, 541-545 (2005).
10. B. H. Cumpston, S. P. Ananthavel, S. Barlow, D. L. Dyer, J. E. Ehrlich, L. L. Erskine, A. A. Heikal, S. M. Kuebler, I. Y. S. Lee, D. McCord-Maughon, J. Qin, H. Rockel, M. Rumi, X. L. Wu, S. R. Marder, and J. W. Perry, "Two-photon polymerization initiators for three-dimensional optical data storage and microfabrication," Nature **398**, 51-54 (1999).
11. S. Kawata, H. B. Sun, T. Tanaka, and K. Takada, "Finer features for functional microdevices," Nature **412**, 697-698 (2001).

#75453 - $15.00 USD Received 26 September 2006; revised 20 October 2006; accepted 20 October 2006

12. J. Serbin, A. Egbert, A. Ostendorf, and B. N. Chichkov, R. Houbertz, G. Domann, J. Schulz, C. Cronauer, L. Fröhlich, and M. Popall, "Femtosecond laser-induced two-photon polymerization of inorganic-organic hybrid materials for applications in photonics," Opt. Lett. **28**, 301–303 (2003).
13. M. Deubel, G. Von Freymann, M. Wegener, S. Pereira, K. Busch, and C. M. Soukoulis, "Direct laser writing of three-dimensional photonic-crystal templates for telecommunications," Nat. Mater. **3**, 444-447 (2004).
14. J. Serbin, and M. Gu, "Experimental evidence for superprism effects in three-dimensional polymer photonic crystals," Adv. Mater. **18**, 221-224 (2006).
15. J. Serbin, and M. Gu, "Superprism phenomena in waveguide-coupled woodpile structures fabricated by two-photon polymerization," Opt. Express **14**, 3563-3568 (2006).
16. P. Lodahl, A. F. Van Driel, I. S. Nikolaev, A. Irman, K. Overgaag, D. Vanmaekelbergh, and W. L. Vos, "Controlling the dynamics of spontaneous emission from quantum dots by photonic crystals," Nature **430**, 654-657 (2004).
17. G. R. Maskaly, M. A. Petruska, J. Nanda, I. V. Bezel, R. D. Schaller, H. Htoon, J. M. Pietryga, and V. I. Klimov, "Amplified spontaneous emission in semiconductor-nanocrystal/synthetic-opal composites: Optical-gain enhancement via a photonic crystal pseudogap," Adv. Mater. **18**, 343-347 (2006).
18. R. D. Schaller, M. A. Petruska, and V. I. Klimov, "Tunable near-Infrared optical gain and amplified spontaneous emission using PbSe nanocrystals," J. Phys. Chem. B **107**, 13765-13768 (2003).
19. S. Hoogland, V. Sukhovatkin, I. Howard, S. Cauchi, L. Levina, and E. H. Sargent, "A solution-processed 1.53 μm quantum dot laser with temperature-invariant emission wavelength," Opt. Express **14**, 3273-3281 (2006).
20. S. G. Johnson, and J. D. Joannopoulos, MIT Photonic Bands software, http://ab-initio.mit.edu/mpb, 1999.
21. A. L. Campillo, J. W. P. Hsu, C. A. White, and A. Rosenberg, "Mapping the optical intensity distribution in photonic crystals using a near-field scanning optical microscope," J. Appl. Phys. **89**, 2801-2807 (2001).
22. E. Flück, N. F Van Hulst, W. L. Vos, and L. Kuipers, "Near-field optical investigation of three-dimensional photonic crystals," Phys. Rev. E **68**, 56011-156014 (2003).

1. Introduction

With the advance of modern micro-fabrication technology, various types of three-dimensional (3D) photonic crystals (PCs) with complete or partial photonic band gaps (PBGs) in the visible or near-infrared (NIR) wavelength region have been developed [1-9]. Among them, 3D woodpile PCs fabricated by the two-photon polymerization (2PP) method have been studied extensively [7, 9-14] for their great flexibilities and high resolution [11, 12]. Especially, the recent experimental evidence of the superprism effect in polymer PCs demonstrates their great potential to directly serve as functional micro-optical devices in the NIR wavelength region [14, 15]. Moreover, it is relatively easy for polymers to incorporate with active media like quantum dots (QDs), and thus to transform the 3D polymer PCs to active devices by engineering the linear or nonlinear optical properties of the incorporated materials through photonic band effects. Recently, colloidal semiconductor QDs, as promising candidates for their readily tunable emission properties, have been infiltrated into 3D inverse opal PCs for the investigation into their radiation properties in the visible wavelength region [16, 17]. Although QDs with emission in the NIR have been recently developed for next generation photonic devices in telecommunication wavelengths [18, 19], direct-laser fabrication of 3D PCs in the polymer resin doped with NIR QDs has not been explored.

In this paper, we demonstrate, for the first time, the feasibility to incorporate PbSe QDs into 3D woodpile PCs by fabricating the PCs in a commercial QD composite. The 3D QD-doped PCs were fabricated by using the 2PP technique and PBGs with a suppression rate of ~50% in the stacking direction have been observed in the NIR wavelength region. A scanning near-field optical microscope (SNOM) was employed to characterize the woodpile structures. The detailed local intensity distribution in the woodpile structures provided the useful additional information about their optical properties, which is important for optimizing the fabrication process.

2. Two-photon polymerization of PbSe QD composite

The 2PP technique [10-12] we used is a direct laser-writing method, which has been employed successfully in the 3D PC fabrication with various popular commercial photosensitive resins, such as SCR [7], SU-8 [13] and ORMOCER [14]. In 2PP, the

#75453 - $15.00 USD Received 26 September 2006; revised 20 October 2006; accepted 20 October 2006

photosensitive resin is polymerized by irradiation with tightly focused, femtosecond laser pulses (~ 100 fs) at a wavelength that is above the single-photon absorption wavelength, which allows the laser beam to focus into the volume of the resin without having any single-photon-induced polymerization reactions. The size of the polymerized volume can be controlled by the variation of laser power and irradiation time and can be as small as 120 nm [11] when fabricated near the threshold of two-photon absorption. In principle, any arbitrary 3D microstructure within the resolution can be fabricated by scanning the laser focus three-dimensionally within the resin.

The QD composite we used in this work was a commercial PbSe QD composite bought from Evident Technologies (1550 nm Java PbSe Core Shell Evidots in UV Curable Sol-Gel with a concentration of 5 mg ml^{-1}). The PbSe QDs had a peak absorption at wavelength 1537 nm and a peak emission at wavelength 1600 nm. Before fabrication, the PbSe QD composite was dropped onto a coverslip and heated in an oven for 10 minutes at a temperature of 70 ^{o}C. The pre-baked resin was then sandwiched by another coverslip and fixed to a computer controlled piezoelectric-driven nano-scanner (PI, 200 μm × 200 μm × 200 μm) for fabrication. In the fabrication system [7, 14], we used an optical parametric oscillator (Coherent Mira OPO) at a wavelength of 580 nm, a repetition rate of 76 MHz and a pulse duration of ~200 fs. The pulses were focused into the resin with an oil immersion objective [Olympus, numerical aperture (NA) =1.4, 100×]. The threshold for 2PP with this QD composite was ~3.25 mW before the aperture of the objective and 3D structures can be well-developed with irradiation power above 4.5 mW with a scanning speed of 50 μm/s. Under such a low power level, no degradation of QDs was observed. After the polymerization process, the sample was washed in methanol for ~1 minute and rinsed with isopropanol for ~1.5 minutes to remove the unpolymerized resin. The developed sample was then illuminated by a UV lamp for 30 seconds to strengthen the structure. Due to the low volume fraction ratio of QDs (~0.06% calculated from the concentration), no noticeable influence of QDs on the 2PP process has been observed during the experiments. The refractive index of the polymerized QD composite was measured to be 1.494 ± 0.002 by using the traditional Becke line method with a serial of refractive index liquids (Cargille Laboratories).

3. 3D woodpile QD-doped PCs fabricated with 2PP

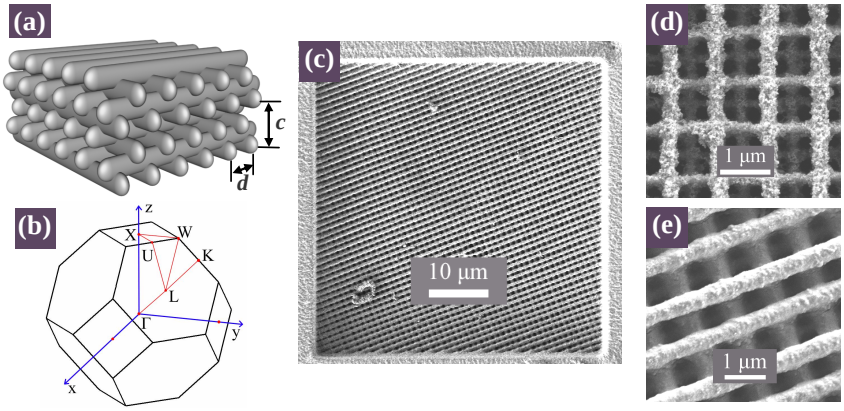

Fig. 1. (a). Sketch of a woodpile structure fabricated with 2PP. (b) The first Brillouin zone of the woodpile structure. (c) SEM image of a 50 μm × 50 μm ×13.5 μm 3D woodpile PC with a solid frame to support the structure. (d) SEM image of polymerized rods with rough surfaces after improper post processing. (e) SEM image of smooth rods after proper post processing.

As shown in Fig. 1(a), the 3D woodpile PC consists of layers of one-dimensional rods with a stacking sequence that repeats itself every four layers. Within each layer, the axes of the rods

#75453 - $15.00 USD Received 26 September 2006; revised 20 October 2006; accepted 20 October 2006

are parallel to each other with a period of *d*. The adjacent layers are rotated by 90° and the rods in every other layer are shifted relative to each other by *d/2*. Generally, the resulting structure has a face-centered tetragonal (fct) lattice symmetry. When the height of the four layers (*c*) and the layer spacing of each layer (*d*) satisfy the special case of $c/d = \sqrt{2}$, the lattice symmetry of the structure is face-centered cubic (fcc). As shown in the unit cell of the reciprocal lattice (the first Brillouin zone) in Fig. 1(b), the ΓX direction represents the stacking direction of the woodpile structure. Figure 1(c) shows the SEM image of a 3D woodpile QD-doped PC with an fct lattice fabricated by means of 2PP. To prevent the structure from collapsing and to minimize the polymer shrinkage during the post development, a solid frame was fabricated around the woodpile structure [7].

The post treatment after the polymerization process is critical for fabrication of high quality woodpile structures in the QD composite with good PBGs. In some circumstance, due to improper post processing, the embedded QDs may cause rough surfaces [see Fig. 1(d)] of the structure, leading to the disappearance of the PBG which may exist for structures with smooth surfaces for the same lattice parameters. The problem can be improved by carefully optimizing the post processing, such as controlling the time for washing and rinsing. As shown in Fig. 1(e), the structure with smooth rods can be realized by increasing the washing time to ~1.5 minutes compared to ~1 minute used for the structure shown in Fig. 1(d).

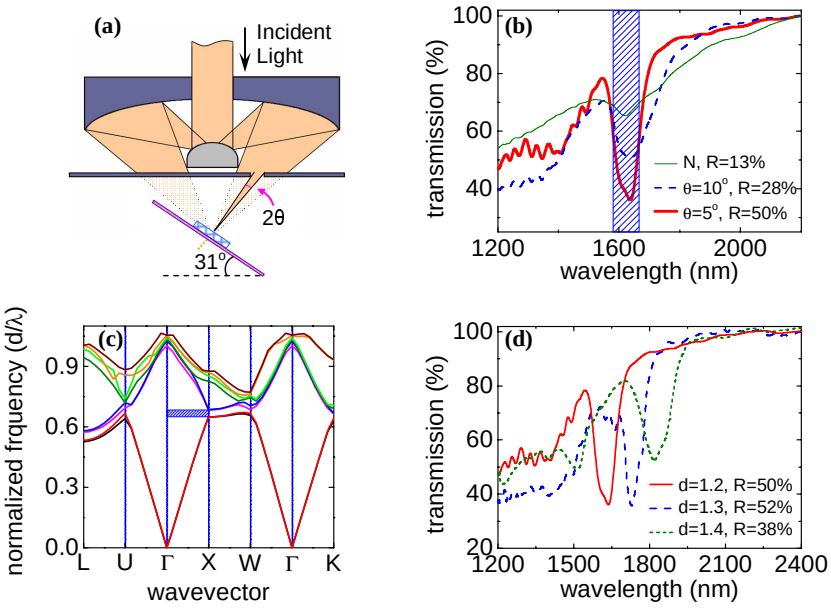

Fig. 2. (a). Sketch of the reflective objective of FTIR with a pinhole setup for the measurement of PBGs. The pinhole provides a confined light cone with a half angle of θ. (b) Transmission spectra of a 3D QD-doped PC measured in the stacking direction with different confined angles. [N means no pinhole being used. R, suppression rate after baseline correction. Spectra were translated along y-axis to 100% at 2200 nm. The shadow area corresponds to the calculated PBG as Fig. 2(c).] (c) Calculated band structure of the woodpile PC with an fct lattice (n=1.494) by using the free MPB software package [20]. The shadow area indicates the PBG in the stacking direction, i.e., the ΓX direction. (d) Transmission spectra of 3D QD-doped PCs with different lattice constants measured in the stacking direction with θ=5°.

Due to the low refractive index of the polymerized QD composite, the fabricated crystals did not possess a complete PBG. Nevertheless, 3D PCs with partial PBGs can also find applications in photonics [14, 15]. In this paper, we mainly investigate the partial PBGs around the stacking direction. The transmission spectra of the fabricated 3D QD-doped PCs

#75453 - $15.00 USD Received 26 September 2006; revised 20 October 2006; accepted 20 October 2006

were measured by using a Fourier-transform infrared (FTIR) spectrometer (Thermo Nicolet) in conjunction with an infrared microscope (Continuum). The reflective objective of the microscope (Reflechromat, 32×, NA=0.65) provides a hollow light cone varying from 18^o to 41^o [see Fig. 2(a)]. To measure the PBG in the ΓX direction accurately, a wedge with an angle of 31^o was used to tilt the sample and a small pinhole was placed in front of the objective to confine the measurement with a half angle of θ [see Fig. 2(a)].

Because the partial PBGs are directional, the size of the pinhole, i.e., the size of the confined angle, influences the transmission spectra significantly. The minimum angle of confinement determines the maximum transmission suppression rate [shown in Fig. 2(b)]. When the measurements were performed with a half angle of 5^o, 10^o and without the pinhole, the suppression rate of the PBG decreased from ~50% to ~28% and ~13%, while the gap/midgap ($\Delta\omega/\omega$) ratio of PBG increased from ~11% to ~15% and ~23%, accompanying with a blue shift of the midgap wavelength from 1636.8 nm to 1636.3 nm and 1621.4 nm. This phenomenon can be explained by the calculated PBG structure in Fig. 2(c). Because we measured the PBGs around the stacking direction [noted by the shadow area in Fig. 2(b) and Fig. 2(c)], the position of the PBG could be slightly shifted towards the shorter wavelength when the measured direction deviated from the ΓX direction towards, for example, the ΓW direction. If the range of the detection angle increased, the measured transmission spectra could include PBG information from multiple directions rather than in a single direction. The effects of overlapped PBGs finally resulted in the broadening of the PBG and the decreasing of the suppression rate in the transmission spectra. Therefore, a small confined angle needs to be employed for measuring the partial PBG accurately. Another thing needs to be pointed is that the size of confined angle should be chosen under the precondition that the Airy disk diameter of the pinhole setup is less than the lateral size of the sample. Figure 2(d) shows the transmission spectra of three different 3D QD-doped PCs measured with the confined angle of 5^o. With lattice constants of 1.2 μm, 1.3 μm and 1.4 μm, the three woodpile PCs show partial band gaps at 1637 nm, 1728 nm, and 1818 nm, respectively. The band gaps of the former two PCs have suppression rates of ~50%.

The suppression rate and the width of the band gaps in the QD-doped PC were comparable with those in the PCs made with ORMOCER [12, 14], an undoped photosensitive resin similar to the host UV-curable sol-gel in the used composite, when the same geometry was used. Further, the midgaps of the QD-doped PCs were located in the wavelength shorter than those of the undoped PCs, mainly due to the higher refractive index of ORMOCER (~1.56 [14]).

4. Characterization of 3D woodpile structures with SNOM

While the band gap structures measured with an FTIR device reveal the optical properties of PCs in the far-field region, a SNOM provides the ability to map the optical intensity distributions near a PC through collecting the optical information in the evanescent field region (~10 nm from the surface of the PC) [21, 22]. Moreover, the understanding of the relationship between the topography structures and the optical functionality obtained by a SNOM provides a direct feedback for the optimization of a fabrication process.

Figure 3 shows the topography and optical signals recorded simultaneously with a SNOM head (NT-MDT) with a 633 nm illumination source from a He-Ne laser coupled by an NA=0.6, 40× objective (Olympus). Figures 3(a) and 3(b) show the fabricated woodpile structures with poor quality, which have unwanted resin in the voids between the rods of the structures. The unwanted resin could be formed when the unwashed resin left after improper post processing was polymerized under the UV illumination. When most of the voids were filled with unwanted resin [Fig. 3(a)], the woodpile structures behaved like a grid window which had a near-field transmission pattern like Fig. 3(b). As the unwanted resin was decreased, rods of the woodpile structure became visible [Fig. 3(c)], resulting in the interfered transmission pattern [Fig. 3(d)]. When the woodpile structure was well-developed with a lattice constant of 1.3 μm as shown in Fig. 3(e) [the structure with a pronounced band gap shown in Fig. 2(d)], the optical signal from the SNOM was greatly decreased and the

#75453 - $15.00 USD Received 26 September 2006; revised 20 October 2006; accepted 20 October 2006

transmission pattern became complicated [Fig. 3(f)], which may be caused by various optical functionalities such as the multiple scattering of 633 nm light by the well arranged periodic structures and/or the effect of the higher order photonic band gaps [7, 8]. Thus, synchronous topography and optical signals from the SNOM can provide the useful information for evaluation of the quality of woodpile structures, which in return gives feedback for optimizing the fabrication process.

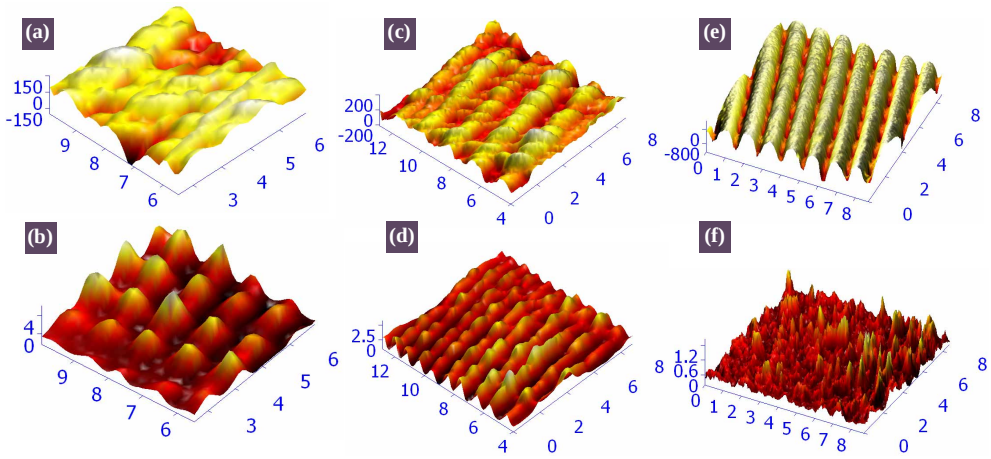

Fig. 3. Topography signals (a, c, e) and optical signals (b, d, f) recorded simultaneously with a SNOM from 3D woodpile structures fabricated with different conditions. (a, b) The voids between the rods were totally filled with unwanted resin. (c, d) The voids between the rods were partially filled with unwanted resin. (e, f) A well-developed woodpile PC with a high quality PBG. Units of x and y axes: μm. Units of vertical z axes: nm (for a, c, e) or a.u. (for b, d, f).

5. Conclusion

In conclusion, by using 2PP, high quality 3D woodpile QD-doped PCs with a PBG suppression rate of ~50% in the NIR wavelength range were fabricated with a commercial PbSe QD composite. An angle-resolved FTIR device revealed the strong sensitivity of the measured transmission spectra. Woodpile structures under different fabrication conditions were characterized by a SNOM, giving a useful feedback for improving the fabrication technique and a new approach to exploring the functionalities of 3D PCs in the telecommunication wavelength region.

Acknowledgment

The authors thank Dr. Jesper Serbin for useful experimental discussions. This work was produced with the assistance of the Australian Research Council (ARC) under the Centres of Excellence program. CUDOS (the Centre for Ultrahigh-bandwidth Devices for Optical Systems) is an ARC Centre of Excellence.

#75453 - $15.00 USD Received 26 September 2006; revised 20 October 2006; accepted 20 October 2006